Geosciences Journal
Vol. 20, No. 2, p. 157 − 166, April 2016
DOI 10.1007/s12303-015-0040-3

Lacustrine hyperpycnal flow deposits after explosive volcanic eruptions, Cretaceous Beolkeum Member, Wido Island, Korea

Yong Sik Gihm *Department of Petroleum Resources Technology, University of Science and Technology, Daejeon 305-350, Republic of Korea*
In Gul Hwang* *Petroleum and Marine Research Division, Korea Institute of Geoscience and Mineral Resources, Daejeon 305-350, Republic of Korea*

ABSTRACT: The Cretaceous Beolkeum Member was formed in a lacustrine environment affected by explosive volcanic eruptions, and hyperpycnal flow deposits are well developed following the eruptions. Beds of hyperpycnal flow deposit are generally less than 25 cm thick and consist of an inversely graded and planar laminated lower part, a poorly-sorted and massive middle part, and a normally graded, planar laminated upper part. An internal erosional surface is common between the lower and middle parts. After explosive volcanic eruptions, subaerial drainage systems would be highly disturbed by deposition of fine-grained and loose pyroclasts. The pyroclasts can easily be remobilized by surface runoff, and the surface runoff evolved into sediment-laden floods with excess density to plunge into the lake, providing favorable conditions for the occurrence of the hyperpycnal flows. Compared with classic models of hyperpycnal flow deposits, predominant planar laminations in the lower and upper parts suggest high fallout rates of suspended sediments from the hyperpycnal flows during initial and late stages of deposition. This implies that the hyperpycnal flows were driven from relatively highly concentrated subaerial floods owing to erodible subaerial conditions following the eruptions. Relatively thinly bedded hyperpycnal flow deposits (<25 cm thick) in comparison with the classic models (1 to 4 m thick) can be attributed to short-lived hyperpycnal flows, arising from the disturbed subaerial conditions following eruptions together with relatively small-scale drainage basins around the lake.

Key words: hyperpycnal flows, planar laminations, pyroclastic density currents, lake, remobilization

1. INTRODUCTION

A hyperpycnal flow is a sediment-laden turbulent underflow and is generated when the density of subaerial discharges (commonly during floods) exceeds that of the standing body of water (lake or sea) which they enter (Mulder et al., 2003). The excess density is largely attributed to suspended sediments in the subaerial discharges, and, hence, the occurrence of hyperpycnal flows is largely controlled by the conditions of the subaerial drainage systems (e.g., gradient, watershed area, and constituent sediments) (Milliman and Syvitski, 1992). Immediately after explosive volcanic eruptions, volcanoes and their surrounding areas are covered with unconsolidated, fine-grained, and poorly-sorted pyroclastic sediments (Cas and Wright, 1987; Smith, 1991; McPhie et al., 1993; Manville et al., 2009). These sediments are characterized by a low infiltration rate, and, if rainfall occurs, surface runoff can drastically be increased, providing favorable conditions for frequent generation of subaerial floods (Major et al., 1996; Pierson et al., 1996). Once flood occurs, the flood can easily gain excess density by entrainment of unconsolidated pyroclastic debris and commonly evolve into hyperconcentrated flows and debris flows (lahar) (Smith and Lowe, 1991). If the floods enter a lake or sea, the excess density allows the floods to transform into hyperpycnal flows. Regardless of the favorable conditions for occurrence of hyperpycnal flows in a standing body of water near volcanoes (Milliman and Syvitski, 1992), modern and ancient hyperpycnal flow deposits around volcanoes are rarely described, and their depositional features are unknown.

The Cretaceous Beolkeum Member was deposited in a lacustrine environment affected by explosive volcanic eruptions. Primary and resedimented pyroclastic deposits are intercalated with lacustrine laminated mudstones, forming syneruptive lithofacies assemblages (SLA-1 to SLA-4) (Gihm and Hwang, 2014). In SLA-1, inferred hyperpycnal flow deposits (stratified, inverse to normally graded tuff) overlie subaqueous pyroclastic density current deposits (massive welded lapilli tuff). The inferred hyperpycnal flow deposits are medium bedded (<25 cm thick) and consist of inverse to normally graded very fine to medium ash. Planar laminations are dominated in lower and upper parts. Classic models of the hyperpycnal flow deposits are, however, very thick bedded (>1 m thick) and shows inverse to normal grading together with alternating occurrence of (climbing) ripple cross-laminations and planar laminations in response to temporal changes in physical conditions of the hyperpycnal flows (Mulder et al., 2003; Plink-Björklund and Steel, 2004; Zavala et al., 2006). Although depositional processes of the inferred hyperpycnal flow deposits are already documented as a part of work for interpretation of depositional history of the Beolkeum Member (Gihm and Hwang, 2014), it is necessary to carefully discuss the contrasting depositional features between the inferred hyperpycnal flow deposits and the classic models in order to improve understanding of phys-

*Corresponding author: ighwang@kigam.re.kr

ical behaviors of hyperpycnal flows after explosive volcanic eruptions.

2. TERMINOLOGY

In this paper, pyroclastic terms such as "tuff" and "lapilli tuff" are applied to the lithofacies composed mainly of fine-grained volcaniclastic sediments formed during explosive volcanic eruptions, regardless of depositional processes (Fisher, 1961, 1966; White and Houghton, 2006). Pyroclastic deposits can be formed by primary volcanic processes (e.g., fallout from eruption column or pyroclastic density currents) or resedimented (secondary) depositional processes (e.g., sediment gravity flows) before lithification of the pyroclastic debris (Fisher, 1961, 1966). Primary pyroclastic deposits can be distinguished from resedimented ones on the basis of heat-induced sedimentary structures, including welded texture, columnar joint, and common occurrence of crystal (alkali feldspar) and pumice. The term "epiclastic" is used for rock fragments originating from already lithified volcanic or volcaniclastic rocks. The "chemical" facies in SLA-1 is used for lithofacies composed mainly of microcrystalline quartz (chert) without organic trace or biogenic structures.

3. GEOLOGIC SETTING

During the Cretaceous, the proto-Pacific Plate obliquely subducted under the Eurasian Plate, resulting in the devel-

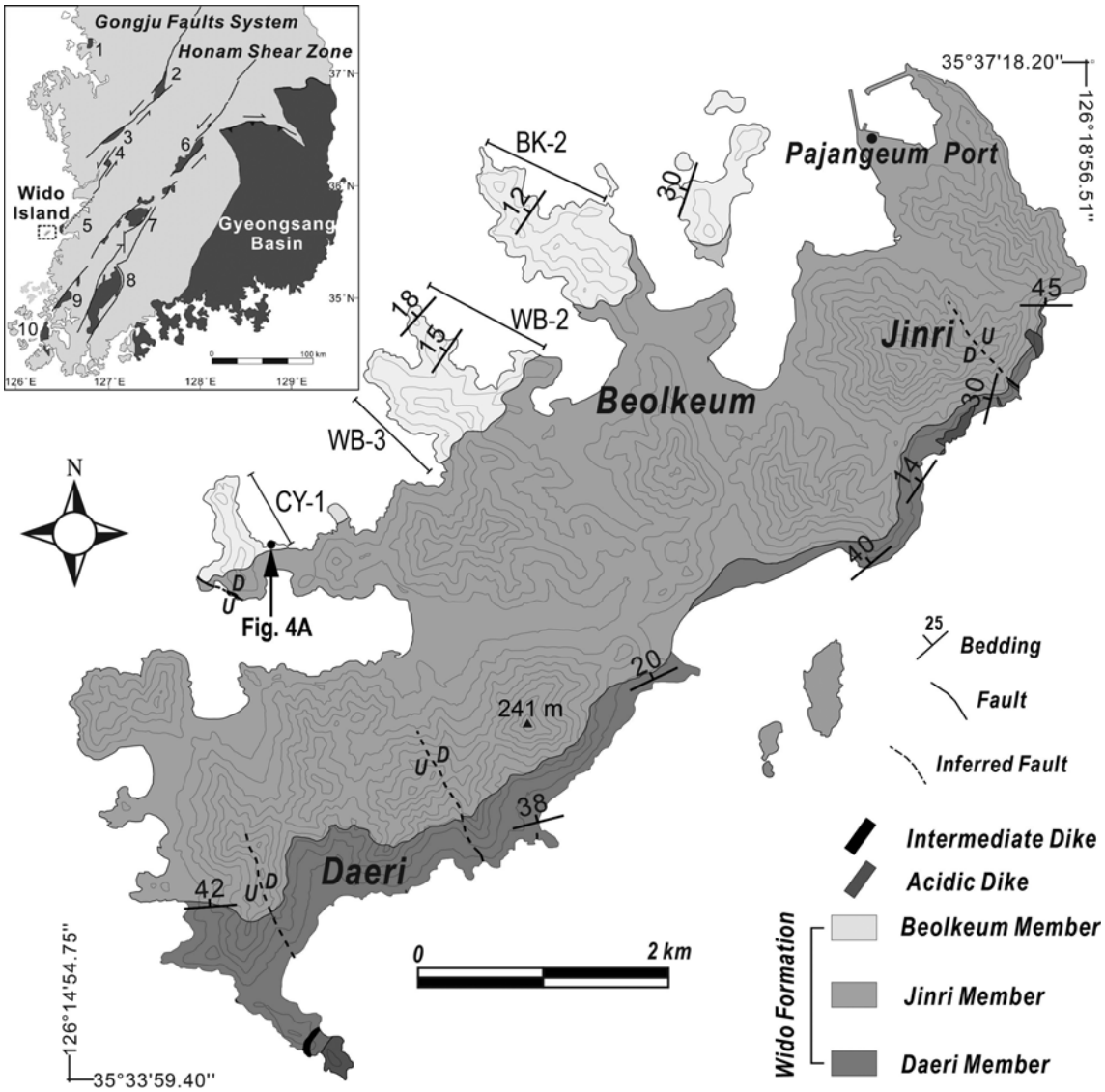

Fig. 1. Distribution of Cretaceous non-marine sedimentary basins in the Korean Peninsula (inset, modified from Chough and Sohn, 2010; Ryang, 2013) and geological map of Wido Island. The Wido Formation is one of the Cretaceous sedimentary successions in the Korean Peninsula and is composed of the Daeri, Jinri, and Beolkeum members (Gihm and Hwang, 2014). Numbers in the inset indicate Cretaceous basins along strike-slip fault systems (1: Sihwa Basin, 2: Eumsung Basin, 3: Kongju Basin, 4: Puyeo Basin, 5: Kyokpo Basin, 6: Yongdong Basin, 7: Jinan Basin, 8: Neungju Basin, 9: Hampyeong Basin, 10: Haenam Basin).

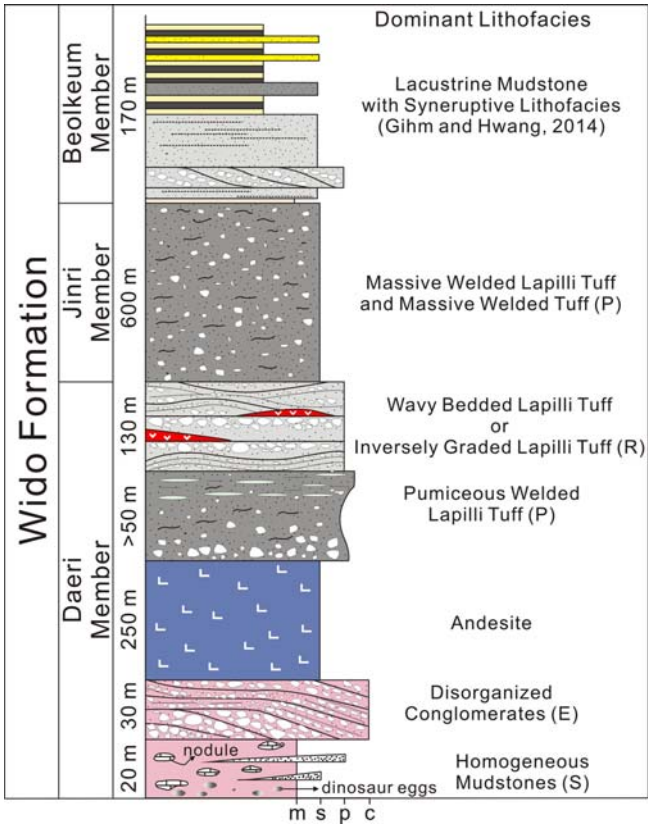

Fig. 2. Schematic stratigraphic log of Wido Formation (P: primary pyroclastic deposit, R: resedimented pyroclastic deposits, E: epiclastic deposits, S: silisiclastic deposits, m: mud, s: sand, p: pebble, c: cobble) (modified from Gihm and Hwang, 2014).

opment of sinistral strike-slip fault systems in the southern part of Korean Peninsula (Chough and Sohn, 2010) (Fig. 1, inset). Many small (<15 (width) × 40 (length) km^2) strike-slip basins were formed along these fault systems and were filled by non-marine sediments (Ryang, 2013). These basins were also affected by effusive and/or explosive volcanic eruptions, and intermediate to felsic lava and tuff are commonly intercalated with the basin-fill sediments (Chough and Sohn, 2010). The Wido Formation exposed on Wido Island is one of the Cretaceous sedimentary successions, which can be divided into the Daeri, Jinri, and Beolkeum members (Figs. 1 and 2). The lowermost Daeri Member consists mainly of andesite and pyroclastic and epiclastic deposits. The Jinri Member is approximately 600 m thick and is composed primarily of rhyolitic, massive welded lapilli tuff and massive welded tuff (Fig. 2), deposited by pyroclastic density currents driven from southwestern part of Wido Island (Gihm and Hwang, 2014). According to age determination using U-Pb ratios in zircon crystals, the Jinri Member was formed at 85.7.1 ± 2.9 Ma (Koh et al., 2013). The overlying Beolkeum Member is exposed in the northwestern part of Wido Island (about 1 km^2) (Fig. 1). The Beolkeum Member is represented by lacustrine laminated mudstones, commonly intersected by small-scale syndepositional normal faults (Figs. 3a and b). The laminated mudstones are intercalated with four syneruptive lithofacies assemblages (SLA-1 to SLA-4) (Gihm and Hwang, 2014), and beds of the inferred hyperpycnal flow deposits are well exposed in SLA-1.

3.1. Depositional History of SLA-1

Syneruptive lithofacies assemblage-1 is composed of four syneruptive lithofacies and one chemical facies and overlain by laminated mudstones (Gihm and Hwang, 2014, Table 1). The lowermost part of SLA-1 is represented by massive welded lapilli tuff (emLT) corresponding to the uppermost part of the Jinri Member. The massive welded lapilli tuff is more than 25 m thick and commonly intruded by a number of dark mud dikes (Fig. 3c), reflecting deposition of the massive welded lapilli tuff on muddy substrate, implying subaqueous entry of parental pyroclastic density currents (Gihm and Hwang, 2014). In addition, in the upper part, the massive welded lapilli tuff is intercalated with thin beds of chert (C) formed by chemical precipitation of silica within standing body of water (Gihm and Hwang, 2014) (Fig. 3d). This is indicative of multiple

Table 1. Descriptions and interpretations of lithofacies in SLA-1 (modified from Gihm and Hwang, 2014)

Facies Code	Lithofacies	Description	Interpretation
emLT	Massive welded lapilli tuff	Composed of poorly-sorted, angular to subangular, lithic lapilli and pumices supported by welded, very fine to fine ash matrix; broken to euhedral alkali feldspar; columnar joints; intruded by numerous mud dikes; intercalated with bedded chert	Pyroclastic density currents entering into a lacustrine environment
mLT	Massive lapilli tuff	Consisting of lithic lapilli and pumices with boulder-sized epiclastic debris; progradational geometry; coarsening-upward trends	Debris flows
Tn	Normally graded tuff	Moderately to well-sorted medium to very fine ash; planar stratifications in the upper part; sharp or erosional boundary	Turbidity currents
sT(i-n)	Stratified, inverse to normally graded lapilli tuff	Medium to very fine ash; inverse to normal grading; internal erosional surface; planar laminations in the lower and upper parts	Hyperpycnal flows
C	Bedded chert	Microcrystalline texture; convolution; lack of biogenic structures	Chemical precipitation of silica in a lake

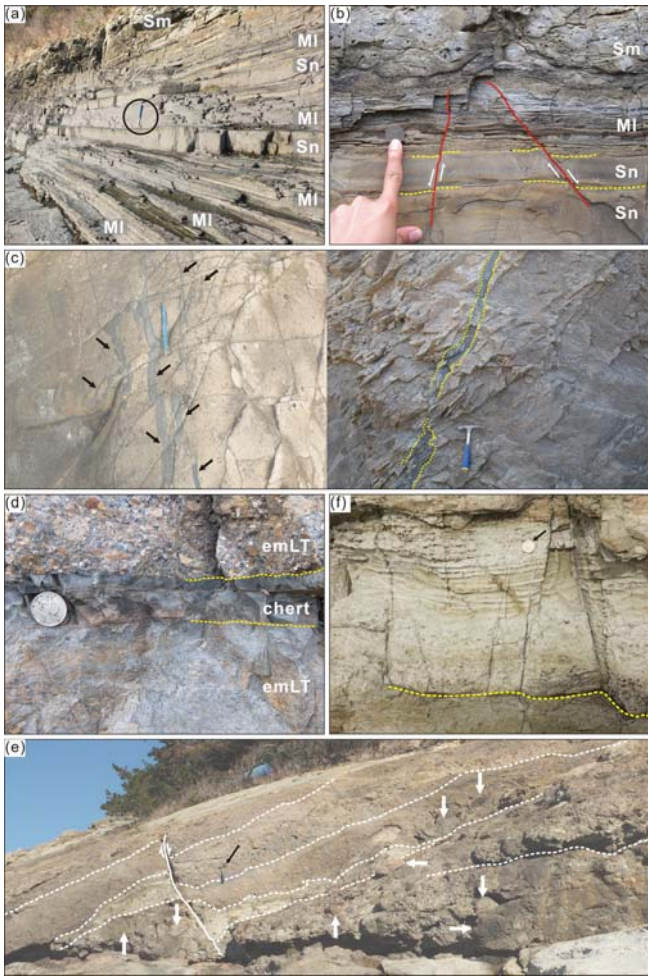

Fig. 3. Photographs of lithofacies in the Beolkeum Member and SLA-1. (a) The Beolkeum Member (lacustrine deposits) is composed of laminated mudstones (Ml) intercalated with normally graded sandstones (Sn, turbidites) and massive sandstones (Sm, debrites). A hammer for scale. (b) Syndepositional normal faults in the Beolkeum Member. (c) Abundant dark mud dikes in the massive welded lapilli tuff in SLA-1. A pencil (14.5 cm long) and hammer for scale (after Gihm and Hwang, 2014). (d) Thin chert beds in the upper part of the massive welded lapilli tuff (emLT). A coin (2.16 cm in diameter) for scale (modified from Gihm and Hwang, 2014). (e) Outcrop view of massive lapilli tuff (debris flow deposits) in SLA-1. Progradational geometry and boulder-sized lithic clasts (white arrows) are noteworthy. A hammer (black arrow) for scale (modified from Gihm and Hwang, 2014). (f) Outcrop view of normally graded tuff deposited by waning turbidity currents in SLA-1. A coin (2.4 cm in diameter) for scale (after Gihm and Hwang, 2014).

emplacements of the pyroclastic density currents into the subaqueous environments (lake) with temporal quiescence (Gihm and Hwang, 2014). The stratified, inverse to normally graded tuff (sT(i-n)) is exposed above the massive welded lapilli tuff, interpreted to have been deposited by hyperpycnal flows (see below for detailed description and interpretation), and passes upwards into massive lapilli tuff (mLT). The massive lapilli tuff was deposited by debris flows and consists of boulder-sized epiclastic debris (andesite and lapilli tuff) supported by a poorly-sorted ash matrix. Beds of the massive lapilli tuff show a progradational geometry and coarsening-upward trend, indicating continuous supply of pyroclastic sediments through debris flows into the lake (Fig. 3e). Overlying normally graded tuff (Tn) was formed by waning turbidity currents. Individual beds of the normally graded tuff are less than 1 m thick, and are stacked more than 20 m with a fining-upward trend, probably resulted from gradual decrease in pyroclastic sediment supply to the lake with time (Fig. 3f). Finally, the pyroclastic deposits are draped by laminated mudstones (Ml) (intereruptive lithofacies) (Gihm and Hwang, 2014).

Because of insufficient fossils and fossils trace and areal limitation, specific water depth and lake dimensions can not be estimated (Gihm and Hwang, 2014). However, thickness of massive welded lapilli tuff (emLT) and massive lapilli tuff (mLT) characterized by progradational geometry suggests that water depth of the lake was more than 40 m deep before deposition of SLA-1. In addition, overlying laminated mudstones and pervasive syndepositional normal faults in the Beolkeum Member suggest that the basin continually subsided together with a decrease in volcaniclastic sediment supply. On the basis of areal distribution of the Beolkeum Member, dimensions of the lake were more than 4.6 km^2.

4. STRATIFIED, INVERSE TO NORMALLY GRADED TUFF

In order to reveal sedimentological features and depositional processes of the stratified, inverse to normally graded tuff, we analyzed the tuff using cm-scale sedimentologic logs in a selected area (CY-1) where the tuff is well exposed (Fig. 1). Beds of the stratified, inverse to normally graded tuff overlie the massive welded lapilli tuff (emLT) (Fig. 4a) and can be subdivided into the lower, middle, and upper parts according to vertical variations in grain size and sedimentary structures (Figs. 4a and b). The lower part is 2 to 15 cm thick on a sharp lower boundary and is composed of inversely graded very fine to fine ash. In the lower part, planar laminations are dominant and can be recognized by alternating layers of fine and very fine ash (Figs. 4b and c). Near the lower boundary, the planar laminae (<1 cm thick) are distinctive and internally massive. The planar laminations become faint upwards with an increase in grain size (up to medium ash) and laminae thickness (up to 2 cm) (Fig. 4c). The middle part (1 to 10 cm thick) overlies the lower part commonly with an internal erosional surface (Fig. 4b). In some cases, the internal erosional surface laterally disappears (Fig. 4d). The middle part consists of poorly-sorted pumices (Fig. 4e) with minor amounts of coarse to very coarse ash-sized lithic clasts, supported by massive medium ash. The pumices are subrounded to rounded and range in size from coarse ash to fine lapilli. The middle part passes upwards into the normally graded upper part (Fig. 4b). The upper part (1 to 10

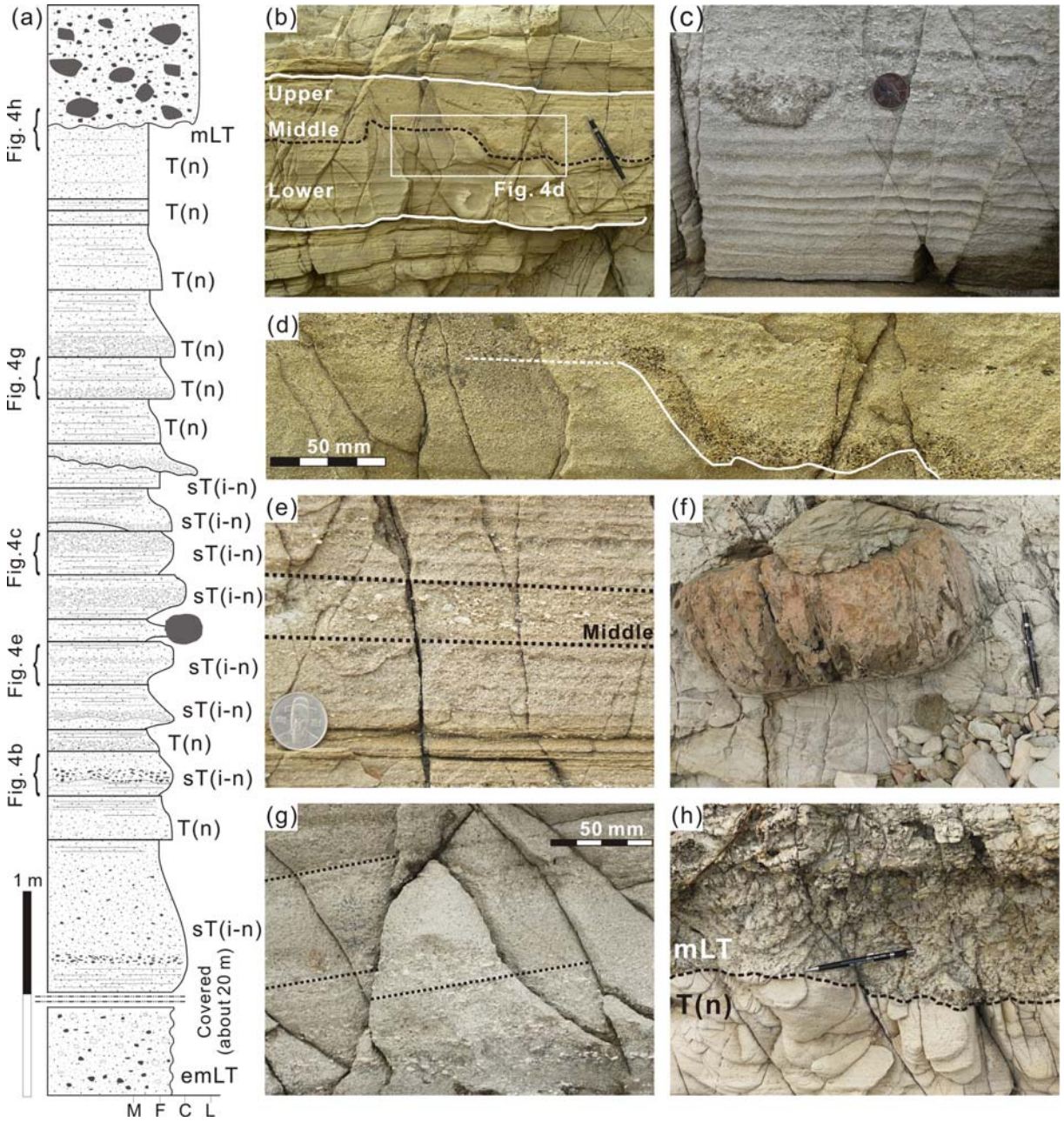

Fig. 4. Stratigraphic log and photographs of stratified, inverse to normally graded tuff. (a) Stratigraphic log of the stratified, inverse to normally graded tuff at CY-1. (b) Outcrop view of the stratified, inverse to normally graded tuff. The stratified, inverse to normally graded tuff consists of a planar laminated and inversely graded lower part, a massive middle part, and a planar laminated and normally graded upper part. A dashed line represents a contact between lower and upper parts. White lines represent bed boundaries (after Gihm and Hwang, 2014). (c) Well-developed planar laminations in the lower part. The planar laminations upwardly become faint with an increase in grain size and thickness of the lamina. (d) Close-up view of the internal erosional surface between lower and middle parts. Note lateral disappearance of an internal erosional surface. (e) Close-up view of pumice-rich, massive middle part. (f) Boulder-sized epiclastic debris (lapilli tuff) in the stratified, inverse to normally graded tuff. (g) Close-up view of normally graded tuff. Note large amounts of pumices and planar laminations (dashed black lines). (h) A contact between normally graded tuff and overlying massive lapilli tuff. Pencils (14.5 cm long) (b, f, and h) and coins (2.4 cm in diameter) (c and e) for scale (emLT: massive welded lapilli tuff, sT(i-n): stratified, inverse to normally graded tuff, T(n): normally graded tuff, mLT: massive lapilli tuff, M: mud, F: fine ash, C: coarse ash, L: lapillus).

cm thick) consists of very fine to fine ash, and planar laminations are also dominant. Thickness of the planar laminations ranges from several mm to 1 cm and decreases upwards. Boulder-sized, rounded epiclastic debris of andesite and lapilli tuff is scattered in the beds (Fig. 4f). The tuff beds range in thickness from 10 to 85 cm thick but are generally less

than 25 cm. In CY-1, the inverse to normally graded tuff beds are overlain by the normally graded tuff and massive lapilli tuff (Figs. 4g and h). The normally graded tuff is composed of medium to very fine ash with pumices, and planar laminations also occur (Fig. 4g).

5. DISCUSSION

5.1. Origin of the Stratified, Inverse to Normally Graded Tuff (sTi-n)

On the basis of abundance of pyroclastic sediments (ash and pumices) in beds of the stratified, inverse to normally graded tuff and lack of intervening sediments (e.g., laminated mudstones) between the tuff (Fig. 4a), it is plausible that the stratified, inverse to normally graded tuff has been deposited by pyroclastic density currents. Variable sedimentary structures and grading patterns in the stratified, inverse to normally graded tuff can be attributed to temporal changes in physical properties (e.g., shear velocity, fallout rates) on a depositional boundary of the pyroclastic density currents (Sohn and Chough, 1989; Druitt, 1998; Valentine and Fisher, 2000; Branney and Kokelaar, 2002). Previous studies suggest that changes in eruption intensity and eruption style during an explosive volcanic eruption directly have influence on the mass flux and velocity of the parental pyroclastic density currents (Cas and Wright, 1987; Brown et al., 2007). In addition, lateral migrations of thalwegs (axes) of the pyroclastic density currents can also result in temporal changes in the physical properties on a depositional boundary (Branney and Kokelaar, 2002). However, rounded to subrounded pumices together with rounded boulder-sized epiclastic clasts within the tuff are indicative of sufficient abrasion before deposition. Relatively well-sorted (very fine to fine ash) and planar laminated natures in the lower and upper parts of the tuff as well as lack of crystals (e.g., alkali feldspar) compared to the underlying massive welded lapilli tuff (emLT, Table 1) are also indicative of hydraulic segregation before and during the deposition. In addition, lack of heat-induced structures (e.g., welded texture) might suggest deposition of the tuff without sufficient heat retention. Based on above evidence, the stratified, inverse to normally graded tuff is interpreted to have originated from resedimentation processes after the eruptions.

Resedimentation processes of the pyroclastic sediments in subaqueous environments can largely be classified into laminar flow (e.g., debris flows), turbulent flows (e.g., turbidity currents), or settling of suspended ash (Cas and Wright, 1987; Mcphie et al., 1993). In case of the stratified, inverse to normally graded tuff, relatively well sorted (very fine to fine ash), planar laminated lower and upper parts, and sharp lower boundary are suggestive of deposition from turbulent flows. The subaqueous turbulent flows can be classified into surge-like turbidity currents (minutes to few hours) and quasi-steady turbidity currents (hours to months) (Kneller and Branney, 1995). Surge-like turbidity currents are formed by rapid release of a finite volume of sediments and composed of a rapidly moving head followed by a relatively slowly moving body and tail (Kneller et al., 1999). Resulting deposits commonly show normal grading with or without planar and/or ripple cross-laminations, depending on physical conditions on a depositional boundary (e.g., fall out rates and shear velocity) (Talling et al., 2012). Quasi-steady turbidity currents commonly originate from the inflowing of subaerial floods into a lake or sea because of their excess density (hyperpycnal flows) and are characterized by initial waxing, quasi-steady, and final waning behavior according to the hydrograph of the floods (Mutti et al., 2003). Therefore, hyperpycnal flow deposits commonly exhibit inverse to normal grading, and an internal erosional surface can be formed during waxing to quasi-steady stages (Mulder et al., 2002). Although the inversely graded division can also be formed by surge-like turbidity currents, previous studies suggest that the inversely graded division is generally thin (<1 cm thick) and formed in a highly concentrated lower part where grain interactions are dominant (Hiscott, 1994). Thus, the inversely graded division formed by surge-like turbidity currents is generally poorly-sorted and contains inversely graded large clasts (Lowe, 1982; Sohn, 1997). In contrast, an inversely graded division of the hyperpycnal flow deposits ranges in thickness from few cm to 1 m (Plink-Björklund and Steel, 2004), depending largely on the duration of the waxing stage (Mulder et al., 2002). Furthermore, gradual fallout of suspended sediments from relatively long duration hyperpycnal flows commonly results in the development of (climbing) ripple cross-laminations and/or planar laminations in the inversely graded division (Mulder et al., 2003).

The relatively thick (<15 cm) and well sorted (very fine to fine ash), inversely graded lower part, overall inverse to normal grading, predominant planar laminations, and internal erosional surface in the stratified, inverse to normally graded tuff suggest a progressive increase and decrease in competence of parental flows and fallout rates of suspended sediments, indicating deposition from hyperpycnal flows. The planar laminations in the lower part could be formed by the collapse of laminar sheared layers of the turbulent flows (Sumner et al., 2008). The laminar sheared layers are near-bed, highly concentrated layers and are moved by shearing driven from overlying turbulent flows. When the friction due to interlocking of particles in the laminar sheared layers exceeds the driving force, the layers would collapse, and planar laminations can be formed. The depositional processes seem to be similar to those of traction carpets, but differ in that grain size segregation (inverse grading) induced by dispersive pressure is negligible (Sumner et al., 2008). Upward disappearance of the planar laminations with a concomitant increase in the laminae thickness suggests an increase in sediment fallout rates accompanied with growing thickness of the laminar sheared layers over a depositional boundary. The massive

middle part containing coarse ash to very coarse ash-sized lithic clasts suggest that the flow had sufficient competence to carry such coarse lithic clasts, but poorly-sorted and massive features point towards hindrance of turbulence over the depositional boundary arising from high fallout rates of suspended sediments (Lowe, 1988). Deposition of large pumices (up to fine lapillus-size) with lithic clasts (coarse to very coarse ash in size) implies that the pumices were saturated by water before the deposition. Internal erosional surface between the lower and middle parts likely represents the highest shear velocity of the flows during the deposition, exceeding threshold for erosion of the medium ash (Zavala et al., 2006). The normally graded and planar laminated upper part represents a decrease in the shear velocity and fallout rates during the deposition. The boulder-sized epiclastic debris may roll or slide and be trapped by the aggrading depositional boundary.

The overlying normally graded tuff seems to have been deposited by surge-like turbidity currents, based on normal grading and planar laminations. The turbidity currents probably resulted from subaqueous remobilization of pyroclastic debris (McPhie et al., 1993) or from (surface?) flow transformation from debris flows depositing the overlying massive lapilli tuff (Fisher, 1983; Sohn, 2000). Alternatively, the normally graded tuff may also be deposited by hyperpycnal flows on the basis of similar grain size and composition of constituent sediments to the underlying stratified, inverse to normally graded tuff. Absence of the inversely graded lower part would be ascribed to complete erosion of the lower part or bypass of the flows during waxing to quasi-steady stages (Mulder et al., 2003).

5.2. Generation of Hyperpycnal Flows after Explosive Volcanic Eruptions

Numerous studies suggest that sediment yield and hydraulic conditions of surrounding areas of volcanoes are highly disturbed by deposition of fine-grained, unconsolidated ash after explosive volcanic eruptions (Manville et al., 2009 and references therein). Although subaerial lithofacies equivalent to the Beolkeum Member are not exposed, the catchment area of the lake would be covered by unconsolidated pyroclastic debris (ash) deposited likely by co-ignimbrite ash during deposition of pyroclastic density currents (massive welded lapilli tuff, emLT) (e.g., Branney and Kokelaar, 2002). Once rainfall occurred, fine-grained and poorly-sorted ash would give rise to an increase in a surface runoff due to their low infiltration rates (Collins and Dunne, 1986), providing favorable conditions for frequent occurrence of subaerial flood. The floods would easily erode and entrain the unconsolidated ash (Fig. 5). According to a research on channel behaviors at Mt. Pinatubo after 6 years from the 1991 explosive eruption (Hayes et al., 2002), suspended sediment concentrations were more than 80 kg/m^3 even during low discharge rates (less than 10 m^3/s), and the sediment concentration further increased with an increase in discharge rates, suggesting that catastrophic events (e.g., rain storm) would not be needed to generate the hyperpycnal flows. Furthermore, this value exceeds the threshold for the generation of hyperpycnal flows in saline water (1–5 kg/m^3, Parsons et al., 2001), and the threshold may be reduced due to low brine content of lake water. Therefore, once rainfall occurred, small-scale subaerial discharges could entrain voluminous suspended sediments enough to transform into hyperpycnal flows when entering the lake (Fig. 5). In addition, relatively low threshold for generations of hyperpycnal flows may lead to frequent occurrence of the hyperpycnal flows after the volcanic eruptions, probably resulting in lack of intervening sediments (e.g., laminated mudstones) between the stratified, inverse to normally graded tuff.

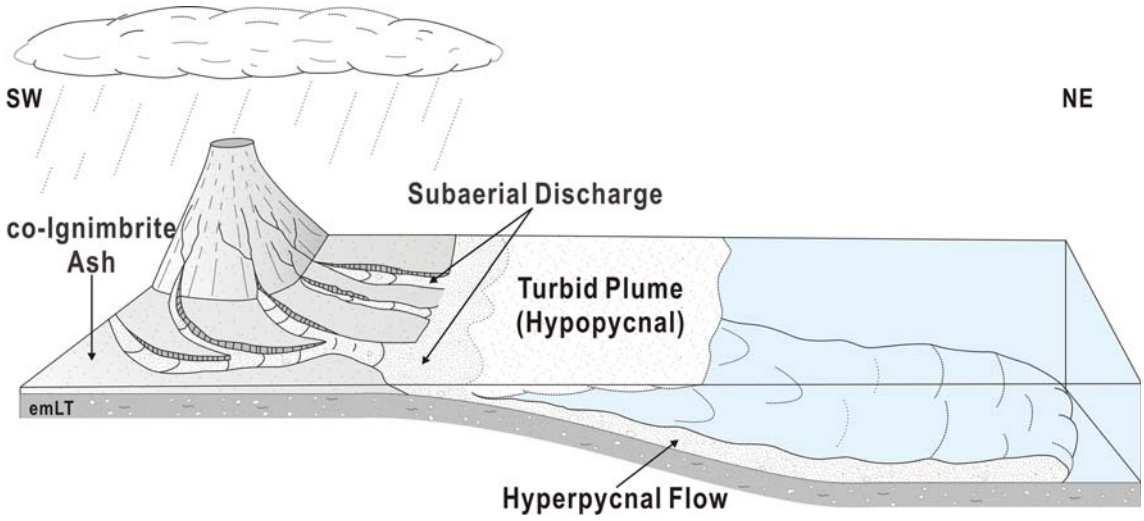

Fig. 5. Schematic depositional model for the hyperpycnal flow after the explosive volcanic eruptions (not to scale) (emLT: massive welded lapilli tuff).

5.3. Comparison between Volcaniclastic versus Non-Volcaniclastic Hyperpycnal Flows

The abundance of the planar laminations is one of the unique depositional features of the hyperpycnal flow deposits in the Beolkeum Member. Previous models of (non-volcaniclastic) hyperpycnal flow deposits suggest that deposition commonly begin with the formation of ripple cross-laminations (Fig. 6a) (Mulder et al., 2003; Zavala et al., 2006). During waxing to quasi-steady stages, the ripple cross-laminations are upwardly transitional to climbing ripple cross-laminations and planar laminations followed by massive sand, reflecting an increase in shear velocity and sediment fallout rates on a depositional boundary. During the waning stage, an opposite tendency can be formed (Fig. 6a). In contrast to the classic models, lower and upper parts of the stratified, inverse to normally graded tuff are predominated by planar laminations (Fig. 6b). Flume experiments show that planar laminations from sediment-laden turbulent flows are formed by freezing of laminar sheared layers under constant conditions of high sedimentation rates (<0.44 mm/s) and high shear velocity (1–1.47 m/s) (66 to 216 μm in grain size from Sumner et al., 2008). On the other hand, low sedimentation rates (0.05 mm/s) and low near-bed shear velocity (<0.9 m/s) are required to form ripple cross-laminations (Sumner et al., 2008). Therefore, in comparison with the classic models, the sediment fallout rates of the hyperpycnal flows was quite high even during initial and late stages of deposition, suggesting that the stratified, inverse to normally graded tuff has been deposited by highly concentrated hyperpycnal flows (up to 35 vol%, Leclair and Arntt, 2005). The high sediment concentration likely resulted from highly concentrated subaerial floods induced by readily erodible subaerial conditions following the eruptions.

According to previous researches, hyperpycnal flow deposits are generally thick (1~4 m), and many authors ascribe their significant thickness to long duration of hyperpycnal flows (Plink-Björklund and Steel, 2004 and references therein) (Fig. 6a). However, in the Beolkeum Member, the stratified, inverse to normally graded tuff is generally less than 25 cm thick (Fig. 6b). As mentioned above, after the explosive volcanic eruptions, disturbed subaerial conditions would allow relatively small surface runoff (less than 10 m^3/s) to transport large amounts of suspended sediments, enough to generate the hyperpycnal flows. In addition, scattered boulder-sized epiclastic debris in the stratified, inverse to normally graded

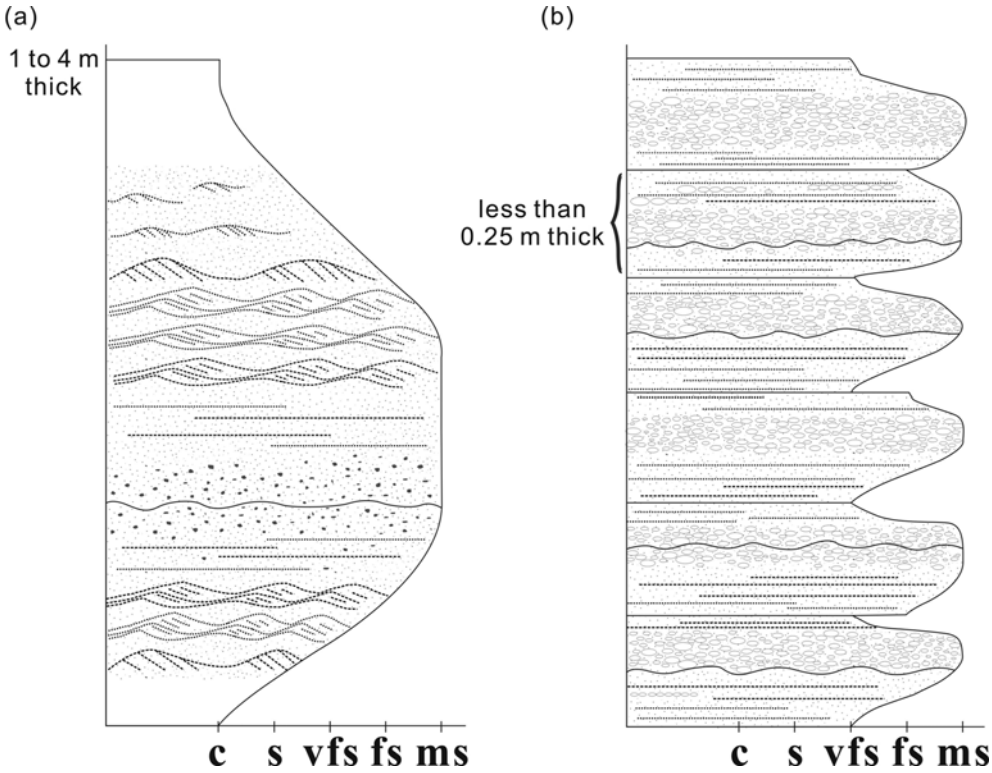

Fig. 6. A comparison between a classical model of (non-volcaniclastic) hyperpycnal flow deposits (modified from Mulder et al., 2003; Zavala et al., 2006) (a) and depositional features of the stratified, inverse to normally graded tuff (b). Beds of the stratified, inverse to normally graded tuff are dominated by planar laminations in the lower and upper parts, indicating high fallout rate of suspended sediments from the hyperpycnal flows during initial and late stage of deposition, implying relatively highly concentrated hyperpycnal flows. Relatively thinly bedded nature is may be due to relatively short-lived hyperpycnal flows, presumably because of highly disturbed subaerial conditions and small-scale drainage basin (c: clay, s: silt, vfs: very fine sand (ash), fs: fine sand (ash), ms: medium sand (ash)).

tuff and in the overlying massive lapilli tuff may indicate that the lake was located adjacent to source volcano(es), implying relatively small-scale drainage basins. The underlying massive welded lapilli tuff formed by subaqueous deposition of hot pyroclastic density currents is also suggestive of proximity between source volcanic edifice(s) and the lake. Thus, once floods occurred, the floods rapidly drained into the lake, and the resulting hyperpycnal flows may inherently be short-lived, forming the relatively thinly bedded hyperpycnal flow deposits.

6. CONCLUSIONS

After the explosive volcanic eruptions, volcanic edifice(s) and surrounding areas would be covered with fine-grained and unconsolidated eruptive materials, offering favorable conditions for the occurrence of frequent subaerial floods. The floods would easily gain excess density to plunge into a lake and evolve into hyperpycnal flows, forming the stratified, inverse to normally graded tuff. In comparison with classic models, the hyperpycnal flow deposits are characterized by numerous planar laminations in the lower and upper parts. This difference is interpreted to be attributed to high fallout rates of suspended sediments during initial and late stages of the deposition. The high fallout rates suggest relatively highly concentrated subaerial floods due to readily erodible subaerial conditions after the eruptions. Relatively small-scale drainage basin around the lake and the highly disturbed subaerial conditions resulted in the occurrence of short-lived hyperpycnal flows, forming relatively thinly bedded (<25 cm thick), hyperpycnal flow deposits.

ACKNOWLEDGMENTS: This study was carried out as a part of the projects (No. GP2013-002-2014) of the Korea Institute of Geoscience and Mineral Resources, financially supported by Ministry of Science, ICT and Future Planning. We thank Professor Y.K. Sohn for constructive discussion in the field. We also appreciate helpful comments of C. Zavala, V. Manville, V. Pascucci, S. Watt, and C. Stevenson to improve previous version of this manuscript. We are grateful to two anonymous reviewers and K. Németh for constructive comments. We also express many thanks to Dr. Chang, T.S. for editorial handling of this manuscript.

REFERENCES

Branney, M.J. and Kokelaar, B.P., 2002, Pyroclastic Density Currents and the Sedimentation of Ignimbrites. The Geological Society of London, Memoir 27, London, 136 p.

Brown, R.J., Kokelaar, B.P., and Branney, M.J., 2007, Widespread transport of pyroclastic density currents from a large silicic tuff ring: the Glaramara tuff, Scafell caldera, English Lake District, UK. Sedimentology, 54, 1163–1190.

Cas, R.A.F. and Wright, J.V., 1987, Volcanic Successions: Modern and Ancient. Allen & Unwin, London, 528 p.

Chough, S.K. and Sohn, Y.K., 2010, Tectonic and sedimentary evolution of a Cretaceous continental arc-backarc system in the Korean peninsula: new view. Earth-Science Reviews, 101, 225–249.

Collins, B.D. and Dunne, T., 1986, Erosion of tephra from the 1980 eruption of Mount St. Helens. Geological Society of America Bulletin, 97, 896–905.

Druitt, T.H., 1998, Pyroclastic density currents. In: Gilbert, J.S. and Sparks, R.S.J. (eds.), The Physics of Explosive Volcanic Eruptions. The Geological Society of London, Special Publication, 145, 145–182.

Fisher, R.V., 1961, Proposed classification of volcaniclastic sediments and rocks. Geological Society of America Bulletin, 72, 1409–1414.

Fisher, R.V., 1966, Rocks composed of volcanic fragments. Earth-Science Reviews, 1, 287–298.

Fisher, R.V., 1983, Flow transformations in sediment gravity flows. Geology, 11, 273–274.

Gihm, Y.S. and Hwang, I.G., 2014, Syneruptive and intereruptive lithofacies in lacustrine environments: The Cretaceous Beolkeum member, Wido Island, Korea. Journal of Volcanology and Geothermal Research, 273, 15–32.

Hayes, S.K., Montgomery, D.R., and Newhall, C.G., 2002, Fluvial sediment transport and deposition following the 1991 eruption of Mount Pinatubo. Geomorphology, 45, 211–224.

Hiscott, R.N., 1994, Traction-carpet stratification in turbidites – fact or fiction? Journal of sedimentary research, 64, 204–208.

Koh H, J., Kwon, C.W., Park, S.I., Park, J.U., and Kee, W.S., 2013, Geological Report of the Julpo, Wido, and Hawangdeungdo Sheets. Korea Institute of Geoscience and Mineralogy Resources, Daejeon, 81 p. (in Korean with English abstract)

Kneller, B.C. and Branney, M.J., 1995, Sustained high-density turbidity currents and the deposition of thick massive sands. Sedimentology, 42, 607–616.

Kneller, B.C., Bennett, S.J., and McCaffrey, W.D., 1999, Velocity structure, turbulence and fluid stresses in experimental gravity currents. Journal of Geophysical Research, 104, 5381–5391.

Leclair, S.F. and Arnott, R.W.C., 2005, Parallel lamination formed by high-density turbidity currents. Journal of Sedimentary Research, 75, 1–5.

Lowe, D.R., 1982, Sediment gravity flows: II. Depositional models with special reference to the deposits of high-density turbidity currents. Journal of Sedimentary Research, 52, 279–297.

Lowe, D.R., 1988, Suspended-load fallout rate as an independent variable in the analysis of current structures. Sedimentology, 35, 765–776.

Major, J.J., Janda, R.J., and Daag, A.S., 1996, Watershed disturbance and lahars on the east side of Mount Pinatubo during the mid-June 1991 eruptions. In: Newhall, C.G. and Punongbayan, R.S. (eds.), Fire and Mud: Eruptions and Lahars of Mount Pinatubo, Philippines. University of Washington Press, Seattle, p. 895–919.

Manville, V., Németh, K., and Kano, K., 2009, Source to sink: A review of three decades of progress in the understanding of volcaniclastic processes, deposits, and hazards. Sedimentary Geology, 220, 136–161.

McPhie, J., Doyle, M., and Allen, R., 1993, Volcanic Textures: A Guide to the Interpretation of Textures in Volcanic Rocks. University of Tasmania, Hobart, 198 p.

Milliman, J.D. and Syvitski, J.P.M., 1992, Geomorphic/tectonic control of sediment discharge to the ocean: The importance of small mountainous rivers. Journal of Geology, 100, 525–544.

Mulder, T., Migeon, S., Savoye, B., and Faugeres, J.C., 2002, Inversely-graded turbidite sequences in the deep Mediterranean. A record of deposits by flood-generated turbidity currents? Reply. Geo-Marine Letters, 22,112–120.

Mulder, T., Syvitski, J.P.M., Migeon, S., Faugéres, J.C., and Savoye, B., 2003, Marine hyperpycnal flows: Initiation, behavior and related

deposits: A review. Marine and Petroleum Geology, 20, 861–882.
Mutti, E., Tinterri, R., Benevelli, G., di Biase, D., and Cavanna, G., 2003, Deltaic, mixed and turbidite sedimentation of ancient foreland basins. Marine and Petroleum Geology, 20, 733–755.
Parsons, J.D., Bush, J.W.M., and Syvitski, J.P.M., 2001, Hyperpycnal plume formation from riverine outflows with small sediment concentrations. Sedimentology, 48, 465–478.
Pierson, T.C., Daag, A.S., Reyes, P.J.D., Regalado, M.T.M., Solidum, R.U., and Tubianosa, B.S., 1996, Flow and deposition of post-eruption hot lahars on the east side of Mount Pinatubo, July–October 1991. In: Newhall, C.G. and Punongbayan, R.S. (eds.), Fire and Mud: Eruptions and Lahars of Mount Pinatubo, Philippines. University of Washington Press, Seattle, p. 921–950.
Plink-Björklund, P. and Steel, R., 2004, Initiation of turbidity currents: Outcrop evidence for Eocene hyperpycnal flow turbidites. Sedimentary Geology, 165, 29–52.
Ryang, W.H., 2013, Characteristics of strike-slip basin formation and sedimentary fills and the Cretaceous small basins of the Korean Peninsula. Journal of the Geological Society of Korea, 49, 31–45. (in Korean with English abstract)
Smith, G.A., 1991, Facies sequences and geometries in continental volcaniclastic settings. In: Fisher, R.V. and Smith, G.A. (eds.), Sedimentation in volcanic settings. Society of Economic Paleontologists and Mineralogists, Special Publication, 45, 109–121.
Smith, G.A. and Lowe, D.R., 1991, Lahars: volcano-hydrologic events and deposition in the debris flow–hyperconcentrated flow continuum. In: Fisher, R.V. and Smith, G.A. (eds.), Sedimentation in volcanic settings. Society of Economic Paleontologists and Mineralogists, Special Publication, 45, 99–106.
Sohn, Y.K., 1997, On traction-carpet sedimentation. Journal of Sedimentary Research, 67, 502–509.
Sohn, Y.K., 2000, Depositional processes of submarine debris flows in the Miocene fan deltas, Pohang Basin, SE Korea, with special reference to flow transformation. Journal of Sedimentary Research, 70, 491–503.
Sohn, Y.K. and Chough, S.K., 1989, Depositional processes of the Suwolbong tuff ring, Cheju Island (Korea). Sedimentology, 36, 837–855.
Sumner, E., Amy, L., and Talling, P., 2008, Deposit structure and processes of sand deposition from decelerating sediment suspensions. Journal of Sedimentary Research, 78, 529–547.
Talling, P.J., Masson, D.G., Sumner, E.J., and Malgesini, G., 2012, Subaqueous sediment density flows: depositional processes and deposit types. Sedimentology, 59, 1937–2003.
Valentine, G.A. and Fisher, R.F., 2000, Pyroclastic surges and blasts. In: Sigurdsson, H. (ed.), Encyclopedia of Volcanoes. Academic Press, San Diego, p. 571–580.
White, J.D.L. and Houghton, B.F., 2006, Primary volcaniclastic rocks. Geology, 34, 677–680.
Zavala, C., Ponce, J.J., Arcuri, M., Drittanti, D., Freije, H., and Asensio, M., 2006, Ancient lacustrine hyperpycnites: A depositional model from a case study in the Rayoso Formation (Cretaceous) of west-central Argentina. Journal of Sedimentary Research, 76, 41–59.

Manuscript received November 18, 2014
Manuscript accepted June 12, 2015